Gibson, G.M., Bowman, R.W., Linnenberger, A., Dienerowitz, M., Phillips, D.B., Carberry, D.M., Miles, M.J., and Padgett, M.J.(2012) *A compact holographic optical tweezers instrument.* Review of Scientific Instruments, 83 (11). p. 113107. ISSN 0034-6748

http://eprints.gla.ac.uk/74528/

Deposited on: 23 January 2013

A compact holographic optical tweezers instrument

G. M. Gibson, R. W. Bowman, A. Linnenberger, M. Dienerowitz, D. B. Phillips et al.

Related Articles

Visual and dynamical measurement of Rayleigh-Benard convection by using fiber-based digital holographic interferometry
J. Appl. Phys. 112, 113113 (2012)

Guide-star-based computational adaptive optics for broadband interferometric tomography
Appl. Phys. Lett. 101, 221117 (2012)

Limits of elemental contrast by low energy electron point source holography
J. Appl. Phys. 110, 094305 (2011)

Cantilever biosensor reader using a common-path, holographic optical interferometer
Appl. Phys. Lett. 97, 221110 (2010)

Extended depth of focus in a particle field measurement using a single-shot digital hologram
Appl. Phys. Lett. 95, 201103 (2009)

Additional information on Rev. Sci. Instrum.

A compact holographic optical tweezers instrument

G. M. Gibson,[1,a)] R. W. Bowman,[1] A. Linnenberger,[2] M. Dienerowitz,[1] D. B. Phillips,[3]
D. M. Carberry,[3] M. J. Miles,[3] and M. J. Padgett[1]

[1]*School of Physics and Astronomy, SUPA, University of Glasgow G12 8QQ, United Kingdom*
[2]*Boulder Nonlinear Systems, 450 Courtney Way, 107 Lafayette, Colorado 80026, USA*
[3]*H. H. Wills Physics Laboratory, University of Bristol BS8 1TL, United Kingdom*

Holographic optical tweezers have found many applications including the construction of complex micron-scale 3D structures and the control of tools and probes for position, force, and viscosity measurement. We have developed a compact, stable, holographic optical tweezers instrument which can be easily transported and is compatible with a wide range of microscopy techniques, making it a valuable tool for collaborative research. The instrument measures approximately $30 \times 30 \times 35$ cm and is designed around a custom inverted microscope, incorporating a fibre laser operating at 1070 nm. We designed the control software to be easily accessible for the non-specialist, and have further improved its ease of use with a multi-touch iPad interface. A high-speed camera allows multiple trapped objects to be tracked simultaneously. We demonstrate that the compact instrument is stable to 0.5 nm for a 10 s measurement time by plotting the Allan variance of the measured position of a trapped 2 μm silica bead. We also present a range of objects that have been successfully manipulated. © *2012 American Institute of Physics.* [http://dx.doi.org/10.1063/1.4768303]

I. INTRODUCTION

Optical tweezers[1,2] are now an established tool for trapping, manipulation, and force measurement of micron sized objects. They use a high numerical aperture (NA) microscope objective lens to produce a gradient force that can tightly trap an object in three dimensions. Optical tweezers systems are available commercially and they have found a number of applications,[3] including measuring the compliance of bacteria,[4] measuring the forces exerted by motor proteins[5,6] and trapping metal nanoparticles.[7,8]

Holographic optical tweezers[9–13] employ spatial light modulators (SLMs), used as dynamic computer-controlled diffractive optical elements, to manipulate many objects independently. They have found many applications including the construction of 3D structures using micron-sized dielectric spheres[14] or living cells[15] and imaging soft cellular surfaces using optically trapped probes.[16]

Careful considerations are required when working with living cells or other light sensitive objects. Near infrared lasers have been successfully used to manipulate living cells as they allow the trapping force to be optimized while minimizing energy absorption.[17] Here we report on the development of a compact holographic optical tweezers system designed for collaborative work outside of the laser laboratory. The system is based on a fibre laser operating at 1070 nm, making it suitable for biological applications,[18,19] and is housed within a custom microscope where only the parts relevant to the non laser specialist are accessible. We have incorporated our own SLM control software, developed using a combination of LABVIEW and OpenGL, which is capable of generating holograms at hundreds of Hz.[20] In ad-

dition, this software is able to use our multi-touch interface, "iTweezers", which simplifies the control of optical tweezers for a number of tasks.[21]

The compact optical layout results in a stable instrument and aberration correction improves the quality of the traps. We verify the stability of the instrument by measuring the Allan variance,[22–24] demonstrating position measurement to an accuracy better than 1 nm for a measurement time between 0.5 and 50 s. The system is compatible with a wide range of microscopy techniques including brightfield, darkfield,[25] stereo,[26] and fluorescence as well as particle tracking using video microscopy.[23,27]

II. SYSTEM CONFIGURATION

A schematic of the optical system is shown in Fig. 1. A Ytterbium fibre laser (IPG Photonics, YLM-5-LP-5C), emitting up to 5 W at 1070 nm with a collimated output of 5 mm diameter, is expanded to fill the aperture of an SLM (Boulder Nonlinear Systems, XY Series). The laser is offset with respect to the second lens of a beam expander such that the upper part of the lens collimates the laser incident on the SLM while the lower part forms the Fourier lens.[28] This results in a more compact optical layout, allowing the optics to be fitted within the footprint of a commercially available *xy* motorized microscope stage (ASI, MS-2000). The laser reflected from the SLM passes a telescope arrangement which images the SLM to the back aperture of a microscope objective (Olympus UApo/340, 40x /1.35).

The microscope stage, in addition to a motorized linear stage (ASI, LS50/M), provides *x,y,z* control over a range of tens of mm, compatible with a wide range of sample holders and objective lenses. The single microscope objective both images the sample and focuses the laser to produce the optical traps. A white LED (Luxeon III Star) coupled through the
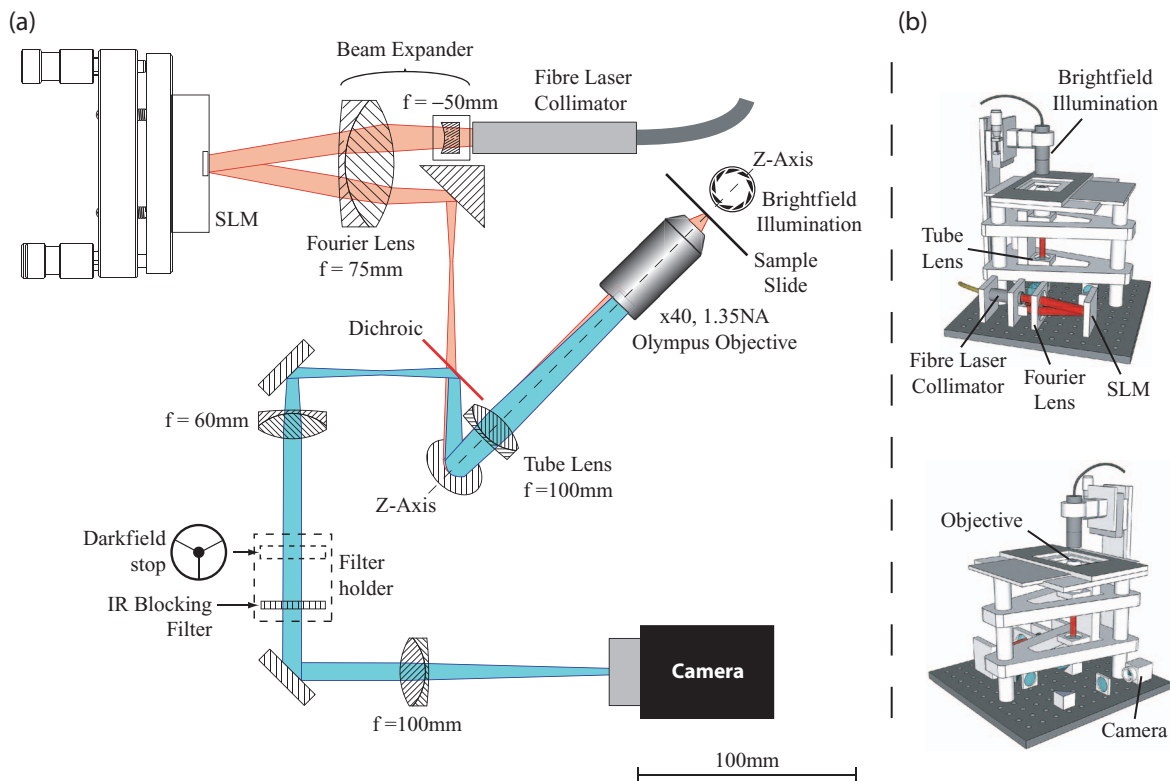
FIG. 1. (a) Schematic of the optical system. The output of the fibre laser is expanded to fill the SLM. The same lens is used both as part of the beam expander and also as the fourier lens after which the laser is coupled into the microscope using a dichroic filter. A reconfigurable filter holder allows the use of laser blocking filters and also the option to insert a center stop for darkfield imaging,[25] wedge prisms for stereo microscopy,[26] or a filter cube for fluorescence imaging. A high speed CMOS camera provides both a live view down the microscope and position tracking of particles. (b) 3D models of the instrument.

microscope condenser, using a short length of acrylic fibre, provides the illumination. The condenser is configured for critical illumination which provides even illumination of the sample from the fibre. Also, using a LED has the advantage that less heat is generated within the microscope and that the driving electronics are more compact. In some applications it is desirable to use darkfield imaging which traditionally requires an objective lens that has a restricted NA. This is unsuitable for 3D optical trapping which requires a high NA objective. In our system we use the standard brightfield illumination from the LED and insert a correctly sized center stop in the Fourier plane of the sample,[25] allowing darkfield imaging which is compatible with the high NA objective used for 3D trapping. In addition, this technique can be used to directly access the scattering spectra of a trapped particle.[25] This center stop can be conveniently placed in the filter holder of the instrument.

A high-speed CMOS camera (Dalsa Genie-HM640) provides a live view down the microscope and can also be used for high-speed particle tracking. At full resolution the camera can acquire images at up to 300 fps. This can be increased by reducing the field of view, allowing particles to be tracked up to a few kHz. For the optical configuration shown in Fig. 1, one camera pixel represents 0.19 μm in the sample. A photograph of the instrument is shown in Fig. 2.

III. SOFTWARE CONTROL

Holograms are generated using our open-source "Red Tweezers" control program,[29] which consists of an OpenGL rendering engine (written in C) and a graphical interface written in LABVIEW. This interface allows the operator to create, move, and delete traps by clicking on a video image of the sample. It is designed to be both easy to use and simple to extend for users that need to customize its operation. The OpenGL Shader Language kernel that renders the holograms is able to be modified from within LABVIEW, making it easy to change the holograms that are rendered. It is also possible to add tabs and plugins to the graphical interface to change the control logic (for example, to effect closed loop control[20, 30]). Image analysis allows us to track the particles in our traps using either centre of mass or a symmetry-based algorithm, implemented as a dynamic-link library (DLL) written in C and called from LABVIEW.[26] Particle tracking is integrated into the graphical interface as shown in Figure 3.

IV. ABERRATION CORRECTION

In an optical tweezers system the presence of aberrations degrade the stiffness of the optical traps.[31] In particular, within our compact system, using the same lens as both part
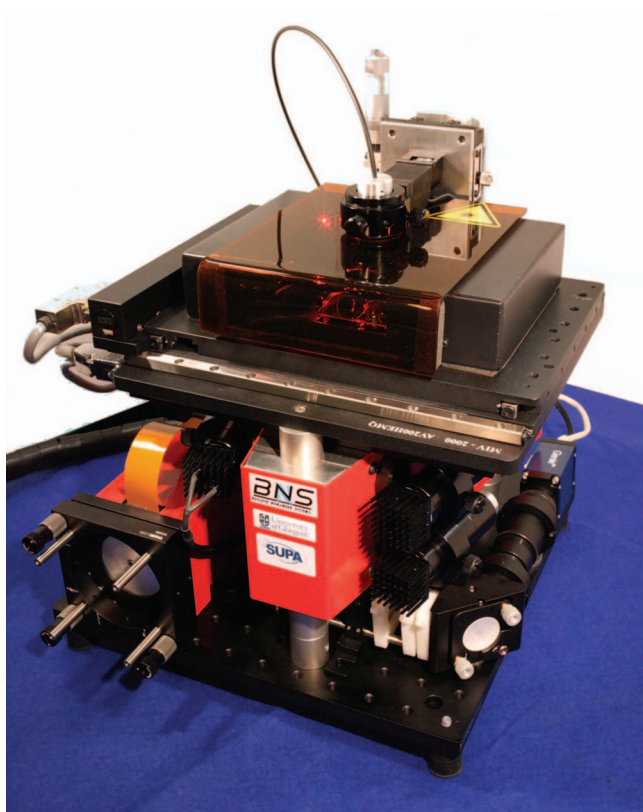
FIG. 2. Photograph of the holographic optical tweezers instrument complete with laser safety shielding. The instrument measures approximately $30\times30\times35$cm. A similarly sized unit contains the driver electronics for the laser, stage, SLM and LED illumination.
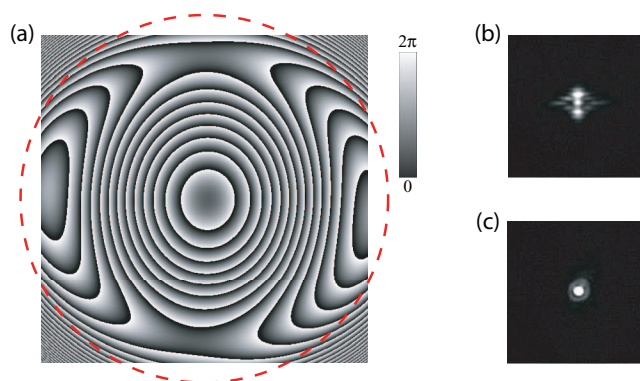

FIG. 4. Correcting for aberrations using the SLM. (a) Phasemap correction applied to the SLM. Note that clipping on the back aperture of the objective lens restricts the effective area of the SLM to the circle shown (dashed red circle). (b) Optical trap shape before correction is applied. (c) Optical trap shape after correction is applied.

beam expander and Fourier lens introduces aberrations which must be corrected. This is especially important when trapping particles that are small compared to the point spread function of the trap[32] and/or trapping deep within the sample.[33] We

take advantage of the fact that the SLM can be used to correct for aberrations, improving the quality of the traps. In addition, the SLM can be used as the principal component of a wavefront sensor either by emulating a Shack-Hartmann sensor,[34] optimizing higher-order modes,[35] or interfering different parts of the SLM.[36,37] We divide the SLM into sub-apertures, each of which is used to project a spot onto a different part of the sample. By tracking the distortion of the array of spots thus formed, we can recover the tilt of the aberration phase surface at each aperture, and hence find the phase pattern corresponding to the aberration. We subtract this phase pattern from the hologram displayed on the SLM to cancel out the aberrations. The first 15 Zernike polynomials serve as a convenient basis set to represent aberrations. Figure 4 shows the aberration correction applied to the SLM along with the improvement in the shape of the optical trap.
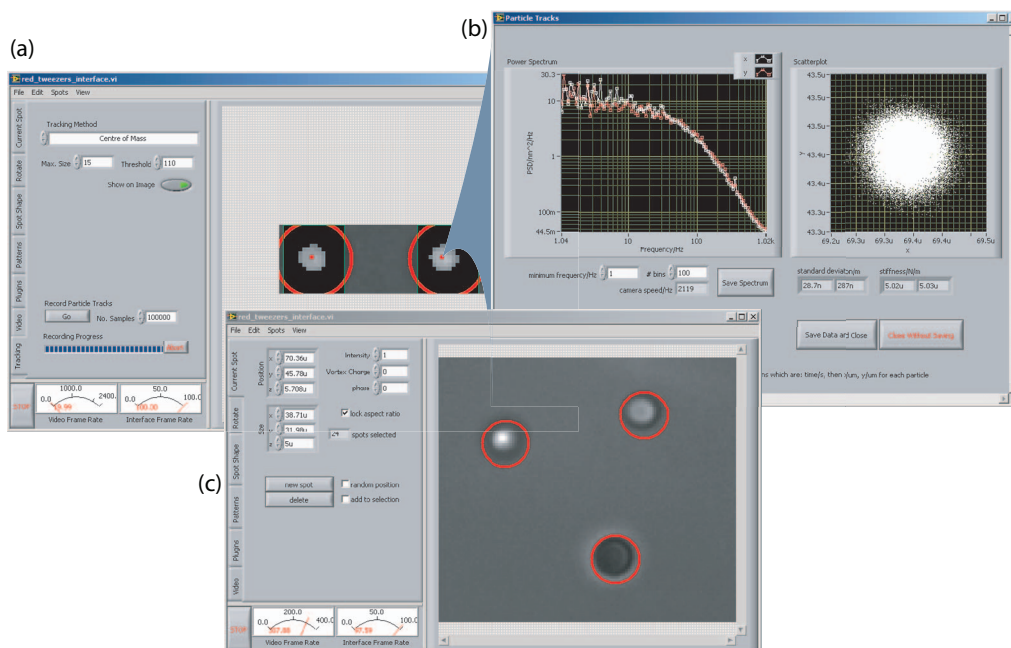

FIG. 3. Control software with integrated particle tracking. (a) Image analysis. (b) Tracked particle data. (c) "Red Tweezers" control panel.
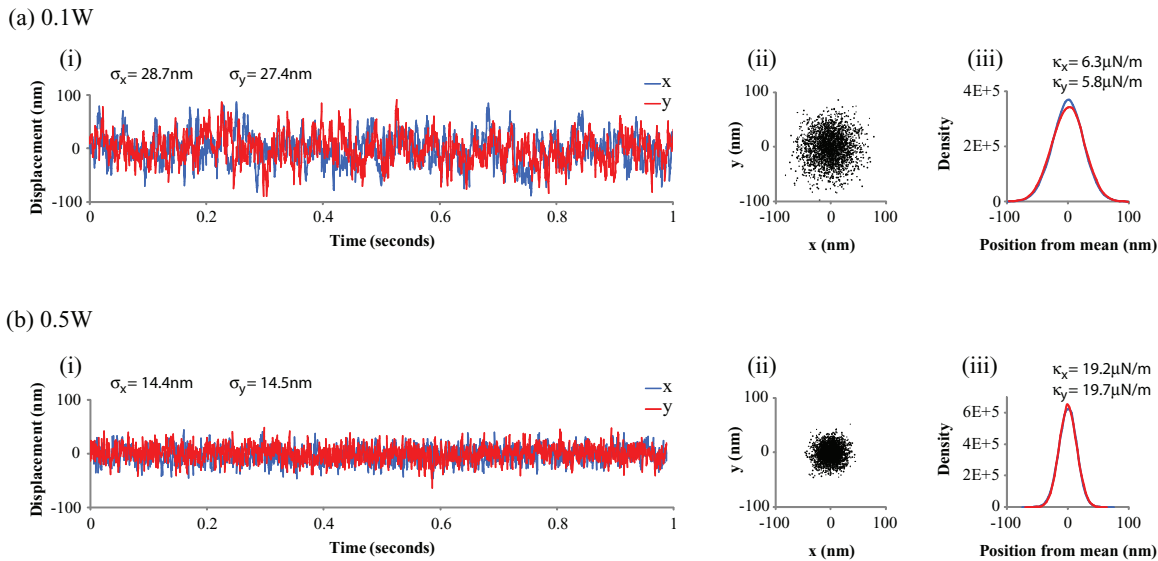
(a) 0.1W

(b) 0.5W

FIG. 5. Position data of a 2 μm silica bead in water using (a) 0.1 W laser output power and (b) 0.5 W laser output power, recorded at 2.4 kHz. (i) Displacement data over 1 s measurement interval with corresponding values for the standard deviations σ. (ii) Scatterplot over 10 s measurement interval (plotting only every 10th point). (iii) Histogram of position measurement over entire data set (approx. 6 min) with corresponding values for the trap strength κ.

V. CHARACTERIZATION

We characterized the optical tweezers instrument by recording and analyzing the position data of a trapped particle. For the purposes of these measurements we placed the instrument on a small air damped optical table in order to isolate the system from environmental sources of noise. The CMOS camera (the main source of heat within the optical layout) was connected to its power supply a few hours before taking measurements in order to maximize thermal stability. We prepared a microscope sample slide containing 2 μm diameter silica beads (Bangs Laboratories, Inc.) in distilled water. We used two laser output powers to trap a single bead, 0.1 W and 0.5 W, respectively. Restricting the field of view of the CMOS camera to approx 5 μm allowed images to be acquired at 2.4 kHz, with the bead position recorded at the same rate, using a center of mass algorithm. Continuous measurements were recorded over a duration of approx. 6 min (900 000 data points) and the data analyzed. Due to the large number of data points recorded, we only plot a subset for the displacement and scatter plots, shown in Fig. 5.

In addition to noise arising from the camera based detector, the trapped particle is subject to Brownian motion and the measurement of its mean position improves with the square root of the averaging time. To demonstrate the stability of the instrument we plot the Allan variance of the bead position given by[23]

$$\sigma_x^2(\tau) = \frac{1}{2}\langle(x_{n+1} - x_n)^2\rangle, \tag{1}$$

where x_n is the average position of the *nth* sample over a time duration τ. This reveals the optimum measurement duration before the measurement is degraded by system drift. The Allan variance of bead position is plotted in Fig. 6. When using the higher laser power the instrument is most stable for measurement times in the 0.5 to 50 s range, showing a stability to better than 1 nm, reaching 0.5 nm for a 10 s measurement.

This is an improvement on what we previously reported[23] for a similar, but much larger, optical tweezers workstation.

Another method of characterizing the system is to record the power spectrum of a trapped bead. Fitting a Lorentzian to the power spectrum of the Brownian motion of the bead[38] reveals the optical trap strength. Figure 7 shows the power spectra for a 2 μm diameter silica bead trapped using 0.1 W and 0.5 W laser output powers.

VI. TRAPPING CAPABILITIES

In Fig. 8 we present a range of objects we manipulated using the optical tweezers instrument. We trapped carbon nanotube clusters, silica beads, yeast cells, and Jurkat cells. By
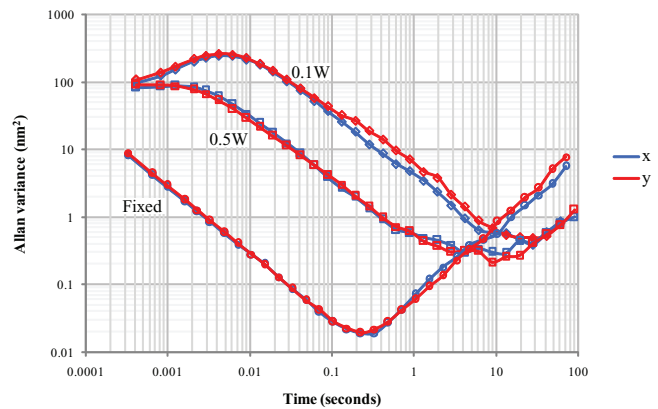

FIG. 6. Stability of position measurement of a 2 μm diameter silica bead for laser output powers of 0.1 W and 0.5 W. In both cases averaging the data over longer time periods improves the accuracy until the Allan variance increases as a result of drift within the system. Plotting the Allan variance of position measurement shows that the instrument can measure displacement to better than 1 nm for a measurement time between 0.5 and 50 s. For comparison, the Allan variance is shown for a 2 μm silica bead fixed to the sample slide coverslip.
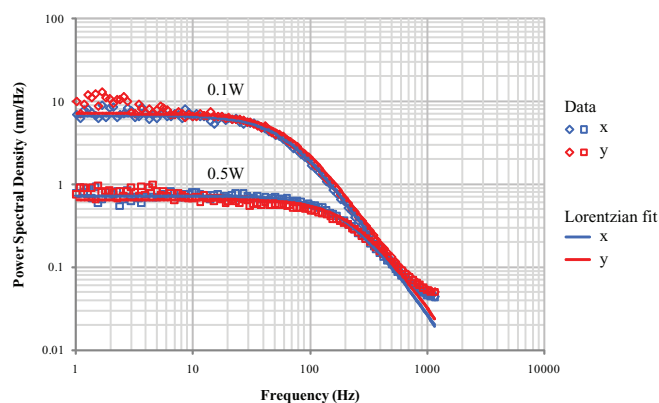
FIG. 7. Power spectra for a 2 μm diameter silica bead trapped using laser output powers of 0.1 W and 0.5 W. Using a laser output power of 0.1 W results in cutoff frequencies $f_{c_x} = 63$ Hz and $f_{c_y} = 67$ Hz, deduced from the Lorentzian fit. Similarly 0.5 W results in $f_{c_x} = 199$ Hz and $f_{c_y} = 229$ Hz. Even at high trap strengths the acquisition frequency is well above the corner frequency of the trapped bead.

hence track, small objects such as the carbon nanotubes, even when trapping many in a cluster. Installing the center stop in the imaging path allowed the nanotube cluster to be easily observed using darkfield imaging, and is compatible with high-speed particle tracking. Large biological samples such as yeast and Jurkat cells were also easily trapped and manipulated. Using an IR laser allowed the cells to be trapped for several minutes without showing apparent signs of cell damage.

It is not always convenient to work with high NA, short working distance objectives such as those commonly used in optical tweezers. Counterpropagating diverging beams can also be used to trap objects by using opposing objective lenses[39,40] or using a dichroic sample slide or mirror behind the sample.[41,42] The scattering forces from a pair of beams cancel when the object is centered axially, removing the requirement for high NA. This enables the use of long working distance objectives at low magnifications. Counter propagating traps can be easily implemented in our system by adopting the dichroic sample slide approach. The SLM is used to create a pair of beams, one of which is reflected by the dichroic to create a backward-propagating focus. The addition of closed loop control of a trapped object can increase the effective trap stiffness to be comparable to that achieved with a single beam gradient trap.[43]

defining multiple traps in 3D we were able to control a custom designed dielectric micro-tool for probing samples. Trapping handles allow the micro-tool to be controlled while keeping the sample clear of the trapping laser.[16] When using standard brightfield imaging it can be difficult to observe, and
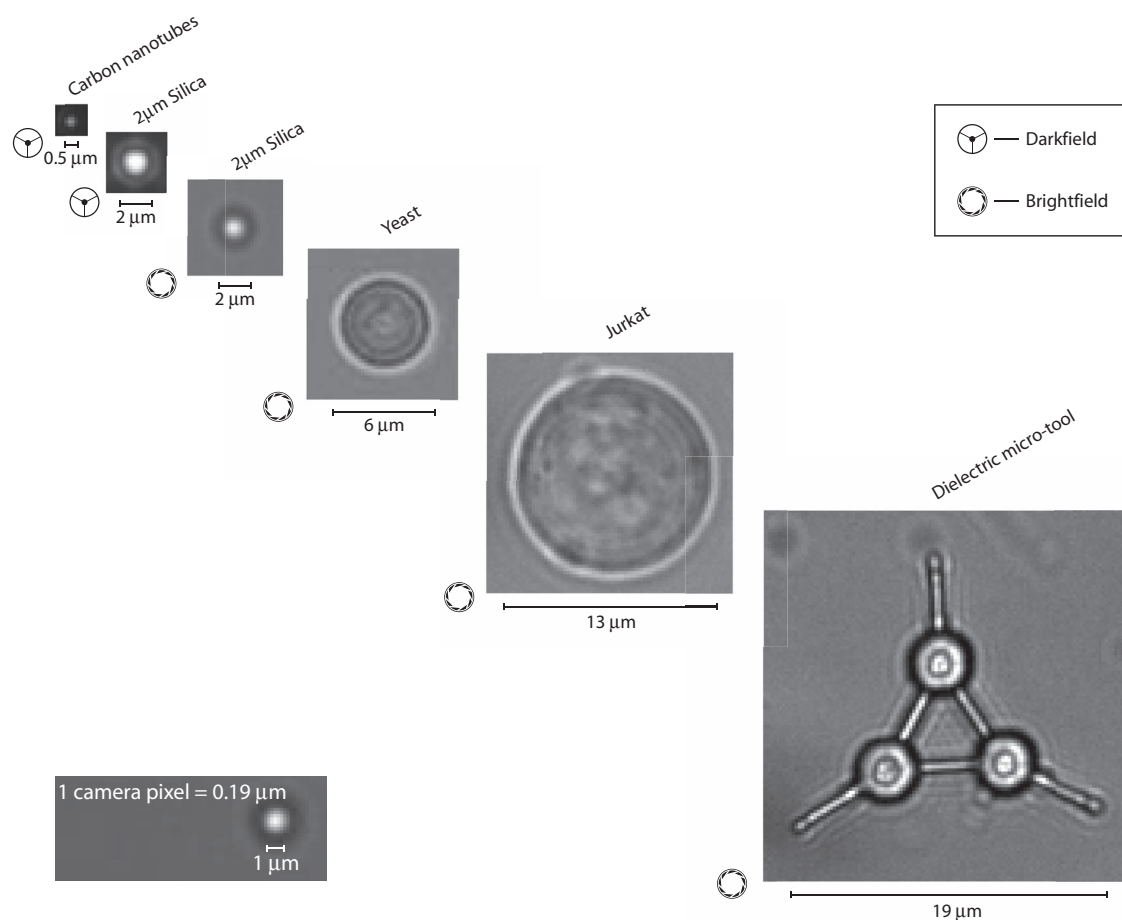

FIG. 8. Gallery showing a selection of different types of object trapped and manipulated using our system. Objects include clusters of carbon nanotubes, living cells, and dielectric micro-tools. Multiple traps can be used for controlling micro-tools in 3D. The option to use darkfield imaging allows clusters of trapped carbon nanotubes to be observed and tracked using a high-speed camera.

VII. CONCLUSIONS

We have developed a compact optical tweezers instrument which can be easily transported and is compatible with a wide range of microscopy techniques and applications. We have shown that the aberration correction applied to the SLM is sufficient to compensate for the optical aberrations introduced by the compact optical layout. This leads to an instrument having a good stability which is similar, and in some cases better, than that of larger optical tweezers workstations. We demonstrated this improved stability by plotting the Allan variance of the position of a trapped silica bead, measured using a high-speed CMOS camera at 2.4 kHz. In addition we demonstrated a range of objects that we manipulated. The use of an IR laser allows living cells to be manipulated without any signs of apparent cell damage. Using a center stop in the imaging path allows us to record darkfield images, and track positions, of objects trapped in 3D using a high NA objective.

ACKNOWLEDGMENTS

[1] A. Ashkin, J. M. Dziedzic, J. E. Bjorkholm, and S. Chu, Opt. Lett. **11**, 288 (1986).

[2] K. C. Neuman and S. M. Block, Rev. Sci. Instrum. **75**, 2787 (2004).

[3] M. Padgett and R. D. Leonardo, Lab Chip **11**, 1196 (2011).

[4] S. M. Block, D. F. Blair, and H. C. Berg, Nature (London) **338**, 514 (1989).

[5] J. T. Finer, R. M. Simmons, and J. A. Spudich, Nature (London) **368**, 113 (1994).

[6] J. E. Molloy, J. E. Burns, J. Kendrick-Jones, R. T. Tregear, and D. C. S. White, Nature (London) **378**, 209 (1995).

[7] P. M. Hansen, V. K. Bhatia, N. Harrit, and L. Oddershede, Nano Lett. **5**, 1937 (2005).

[8] L. Bosanac, T. Aabo, P. M. Bendix, and L. B. Oddershede, Nano Lett. **8**, 1486 (2008).

[9] Y. Hayasaki, M. Itoh, T. Yatagai, and N. Nishida, Opt. Rev. **6**, 24 (1999).

[10] J. Liesener, M. Reicherter, T. Haist, and H. J. Tiziani, Opt. Commun. **185**, 77 (2000).

[11] J. E. Curtis, B. A. Koss, and D. G. Grier, Opt. Commun. **207**, 169 (2002).

[12] D. G. Grier, Nature (London) **424**, 810 (2003).

[13] M. Polin, K. Ladavac, S.-H. Lee, Y. Roichman, and D. G. Grier, Opt. Express **13**, 5831 (2005).

[14] S.-H. Lee and D. G. Grier, Opt. Express **15**, 1505 (2007).

[15] P. Jordan, J. Leach, M. Padgett, P. Blackburn, N. Isaacs, M. Goksör, D. Hanstorp, A. Wright, J. Girkin, and J. Cooper, Lab Chip **5**, 1224 (2005).

[16] D. B. Phillips, J. A. Grieve, S. N. Olof, S. J. Kocher, R. Bowman, M. J. Padgett, M. J. Miles, and D. M. Carberry, Nanotechnology **22**, 285503 (2011).

[17] M. W. Berns, J. R. Aist, W. H. Wright, and H. Liang, Exp. Cell Res. **198**, 375 (1992).

[18] A. Ashkin, J. M. Dziedzic, and T. Yamane, Nature (London) **330**, 769 (1987).

[19] G. J. Brouhard, H. T. Schek, and A. J. Hunt, IEEE Trans. Biomed. Eng. **50**, 121 (2003).

[20] D. Preece, R. Bowman, A. Linnenberger, G. Gibson, S. Serati, and M. Padgett, Opt. Express **17**, 22718 (2009).

[21] R. W. Bowman, G. Gibson, D. Carberry, L. Picco, M. Miles, and M. J. Padgett, J. Opt. **13**, 044002 (2011).

[22] D. W. Allan, Proc. IEEE **54**, 221 (1966).

[23] G. M. Gibson, J. Leach, S. Keen, A. J. Wright, and M. J. Padgett, Opt. Express **16**, 14561 (2008).

[24] F. Czerwinski, A. C. Richardson, and L. B. Oddershede, Opt. Express **17**, 13255 (2009).

[25] M. Dienerowitz, G. Gibson, F. Dienerowitz, and M. Padgett, J. Opt. **14**, 045003 (2012).

[26] R. Bowman, D. Preece, G. Gibson, and M. Padgett, J. Opt. **13**, 044003 (2011).

[27] O. Otto, F. Czerwinski, J. L. Gornall, G. Stober, L. B. Oddershede, R. Seidel, and U. F. Keyser, Opt. Express **18**, 22722 (2010).

[28] V. R. Daria, C. Stricker, R. Bowman, S. Redman, and H.-A. Bachor, Appl. Phys. Lett. **95**, 093701 (2009).

[29] See http://www.gla.ac.uk/schools/physics/research/groups/optics/research/opticaltweezers/software/ for links to our optical tweezers software.

[30] D. B. Phillips, S. H. Simpson, J. A. Grieve, G. M. Gibson, R. Bowman, M. J. Padgett, M. J. Miles, and D. M. Carberry, Opt. Express **19**, 20622 (2011).

[31] Y. Roichman, A. Waldron, E. Gardel, and D. G. Grier, Appl. Opt. **45**, 3425 (2006).

[32] K. D. Wulff, D. G. Cole, R. L. Clark, R. D. Leonardo, J. Leach, J. Cooper, G. Gibson, and M. J. Padgett, Opt. Express **14**, 4169 (2006).

[33] G. Sinclair, P. Jordan, J. Leach, M. J. Padgett, and J. Cooper, J. Mod. Opt. **51**, 409 (2004).

[34] R. W. Bowman, A. J. Wright, and M. J. Padgett, J. Opt. **12**, 124004 (2010).

[35] A. Jesacher, A. Schwaighofer, S. Fürhapter, C. Maurer, S. Bernet, and M. Ritsch-Marte, Opt. Express **15**, 5801 (2007).

[36] I. M. Vellekoop and A. P. Mosk, Opt. Lett. **32**, 2309 (2007).

[37] T. Čižmár, M. Mazilu, and K. Dholakia, Nature Photon. **4**, 388 (2010).

[38] K. Berg-Sørensen and H. Flyvbjerg, Rev. Sci. Instrum. **75**, 594 (2004).

[39] P. J. Rodrigo, V. R. Daria, and J. Glückstad, Appl. Phys. Lett. **86**, 074103 (2005).

[40] P. J. Rodrigo, L. Kelemen, D. Palima, C. A. Alonzo, P. Ormos, and J. Glückstad, Opt. Express **17**, 6578 (2009).

[41] M. Pitzek, R. Steiger, G. Thalhammer, S. Bernet, and M. Ritsch-Marte, Opt. Express **17**, 19414 (2009).

[42] S. Zwick, T. Haist, Y. Miyamoto, L. He, M. Warber, A. Hermerschmidt, and W. Osten, J. Opt. A, Pure Appl. Opt. **11**, 034011 (2009).

[43] R. Bowman, A. Jesacher, G. Thalhammer, G. Gibson, M. Ritsch-Marte, and M. Padgett, Opt. Express **19**, 9908 (2011).